MOLECULAR AND CELLULAR BIOLOGY, Nov. 1992, p. 5206–5216
0270-7306/92/115206-11$02.00/0

Vol. 12, No. 11

Characterization of the Human Immunoglobulin Kappa Gene 3′ Enhancer: Functional Importance of Three Motifs That Demonstrate B-Cell-Specific In Vivo Footprints

JEAN-GABRIEL JUDDE† AND EDWARD E. MAX*

Laboratory of Molecular Immunology, Center for Biologics Evaluation and Research, Food and Drug Administration, Bethesda, Maryland 20892

Received 24 April 1992/Returned for modification 4 June 1992/Accepted 20 August 1992

Using a combination of in vivo footprinting and site-directed mutagenesis, we have functionally characterized an enhancer located 12 kb downstream of the human immunoglobulin kappa constant-region gene. The core enhancer region is highly homologous to the murine 3′κ enhancer. However, in addition to two regulatory elements homologous to the functional motifs of the murine enhancer, we find a third positive regulatory element in the human enhancer. This element is associated with an 11/12-bp direct repeat (DR) that is well conserved in the murine locus but was not recognized as functionally important in the murine enhancer. Mutation of any of the three motifs of the human enhancer decreases its activity to 3 to 20% of the wild-type level, indicating cooperative interaction between these elements. The DR motif does not resemble any known enhancer element and does not appear to function as a transcriptional activator on its own when present in multiple copies. Interestingly, nuclear extracts from both B- and T-cell lines contain factors binding to DR in vitro, but in vivo footprinting shows no evidence of protein-DNA binding in the T-cell line. This finding suggests that an additional regulatory mechanism, such as the effect of chromatin configuration on accessibility, may be involved in the B-cell-restricted activity of the human 3′κ enhancer.

The expression of immunoglobulin (Ig) genes is restricted to cells of the B-cell lineage and represents a model system for the study of tissue-specific gene regulation. Ig κ light-chain expression is regulated at the transcriptional level by a promoter directly upstream of the variable (V)-region gene and an enhancer located in the intron between the joining (J)- and constant (C)-region exons. Recently, an additional enhancer located 8 kb downstream of the C-region gene was described in the mouse (19). How this downstream enhancer functions in conjunction with the other two regulatory elements is still unknown, but experiments with transgenic mice suggest that it plays an important role in κ light-chain expression (20).

While considerable information has been obtained about the function of the Vκ promoter and the κ-intron enhancer and the *trans*-acting factors that modulate their activity (15), much less is known about the regulation of the 3′κ enhancer. Transfection assays have shown that the murine 3′κ enhancer is inactive in pre-B-cell lines and active in mature B-cell and plasma cell lines, a developmental control pattern similar to that of the κ-intron enhancer (30). Two positive regulatory elements have been identified in the core enhancer on the basis of deletion analysis (20) and of the ability of multimerized enhancer fragments to stimulate transcription from a heterologous promoter (30). One of the two elements contains a consensus binding site for the B-cell- and macrophage-specific transcription factor PU.1 and the family of Ets-related proteins (13). The other element contains a binding motif for factors of the helix-loop-helix (HLH) type (12). The 3′κ enhancer region also includes several sequences, such as the κB motif and the interferon response element for which function has not been demonstrated, that are similar to other known enhancer motifs; these sequences could potentially regulate transcriptional activity at a particular stage of B-cell activation or development (19).

We have studied the human sequence homologous to the mouse 3′κ enhancer and find that it also functions as a B-cell-specific enhancer. To characterize enhancer elements precisely, we have combined in vivo footprinting with functional analysis, using a series of mutant enhancers generated by site-directed mutagenesis. Three positive regulatory elements that show B-cell-specific protein binding in vivo have been characterized. Two of these correspond to the PU.1 and HLH-binding motifs found in the mouse enhancer. The third element is an 11/12-bp direct repeat (DR) which has not been identified previously and does not resemble other known regulatory motifs. Although proteins that bind to this repeat element in vitro are present in T cells, the in vivo alterations in dimethyl sulfate (DMS) reactivity in this motif, revealed in B cells by genomic footprinting, are not found in T-cell DNA. This observation may reflect an additional level of regulation, such as altered chromatin conformation, associated with the activity of this enhancer in B cells.

MATERIALS AND METHODS

Plasmid constructions. A 156-bp Vκ gene promoter was derived from the MOPC41 Vκ gene (33) by polymerase chain reaction (PCR), using the following oligonucleotides as primers: 5′-CGGCCGGATCCGTGACCAATCCTAACTGCTTC and 5′-CCGAGATCTGAGTCCTGACTGCAATGACAATG GC. The amplified DNA was cut (at sites designed into the primers) with *Bam*HI and *Bgl*II, and the resulting fragment, along with the bacterial chloramphenicol acetyltransferase (CAT) gene and the simian virus 40 (SV40) splice and polyadenylation sequences, were cloned into the *Cla*I site of a Bluescript KS$^+$ plasmid (Stratagene) in which the *Bam*HI

* Corresponding author.
† Present address: Laboratory of Immunology, National Eye Institute, Bethesda, MD 20892.

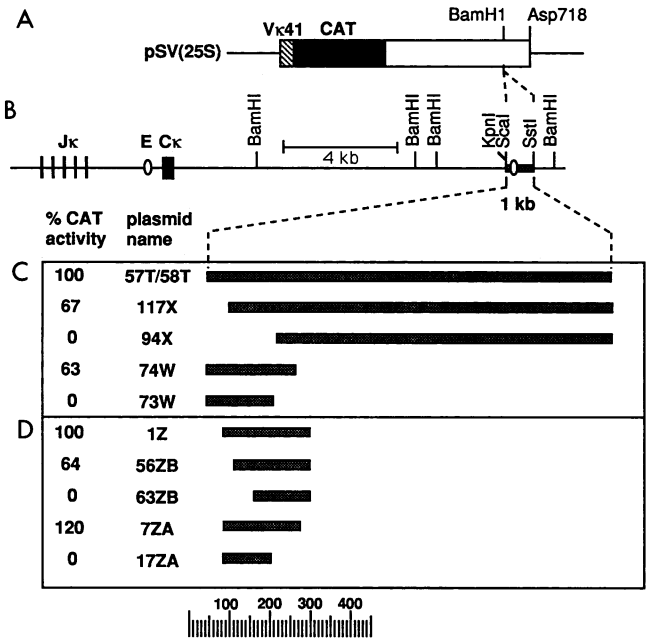

FIG. 1. Constructs defining the boundaries of the human 3'κ enhancer. (A) Diagram of the enhancerless plasmid pVC(25S) that was used as a starting point for constructions. This plasmid has a promoter (derived by PCR from the MOPC41 Vκ gene) inserted upstream of the CAT gene as well as the SV40 splice and poly(A) addition sequences. (B) Human genomic Ig κ locus, including the J regions, the intron enhancer (E), and the Cκ gene. The *Sca*I-*Sst*I fragment from this locus was cloned into the *Bam*HI site of pVC(25S) to yield pVCE(57T), with the enhancer in the normal orientation with respect to transcription and pVCE(58T) in the opposite orientation. CAT activities programmed by plasmids 57T and 58T and terminal enhancer deletion plasmids were tested by transfection in CA46 B cells (C). In a second series of experiments (D), the critical functional segment was synthesized by PCR and inserted between the *Bam*HI and *Asp*-718 sites of pVC(25S), yielding pVCE(1Z), which was actively transcribed. Terminal enhancer deletions of the latter plasmid further delimited the boundaries of functional enhancer sequence. The termini of the enhancer inserts in each construct are as follows, numbered according to the published sequence (22) as indicated by the scale at the bottom of the figure: 57T (5'-30), 117X (5'-97), 94X (5'-213), 74W (30 to 263), 73W (30 to 210), 1A (79 to 296), 56ZB (111 to 256), 63ZB (160 to 296), 7ZA (79 to 273), and 17ZA (79 to 202).

site had been previously destroyed, yielding plasmid pVC(25S). The 1-kb *Sca*I-*Sst*I fragment diagrammed in Fig. 1 was ligated to *Bam*HI linkers and inserted into the *Bam*HI site at the 3' end of the SV40 sequence in both orientations, generating plasmids pVCE(57T) and pVCE'(58T) (Fig. 1). A 218-bp fragment including the presumptive functional enhancer sequences was synthesized by PCR, using plasmid pVCE(57T) as the template and the following primers: upstream (GCGCGGATCCATGCATGCGCGGTTACCGA GTTTCATGGTTACTTGCC) and downstream (GGCCGGT ACCGGGCCCGGCCGTCGACGAAAGGGTGTGGAGTG CTCCACC). The resulting fragment (after digestion of primer sites with *Bam*HI and *Asp*-718) was inserted between the *Bam*HI and *Asp*-718 sites of pVC(25S) to produce plasmid pVCE(1Z). Similarly, a human κ-intron enhancer (0.7-kb *Eco*RI fragment containing the enhancer; *Bgl*II linkered) and an Ig heavy-chain (IgH) enhancer fragment (0.5-kb *Ase*I-to-*Taq*I fragment; *Bam*HI linkered) were inserted into the *Bam*HI site of pVC(25S). To produce plasmids in which the 3'κ enhancer stimulated transcription from the heterologous thymidine kinase (*tk*) and SV40 promoters, plasmid pVCE(1Z) or mutants derived from it were cut with *Asp*-718, blunted with Klenow polymerase, and ligated to *Bgl*II linkers. The DNA fragment containing the enhancer was then cut with *Bam*HI and *Bgl*II, gel purified, and subcloned into the *Bam*HI site downstream of the CAT gene transcribed from an SV40 promoter or upstream of the *tk* promoter in plasmid pBLCAT2 (17).

To make plasmids containing multimers of the DR motif, a double-stranded oligonucleotide representing the DR motif was made with *Bam*HI and *Bgl*II termini. This oligonucleotide was inserted into the *Bam*HI and *Bgl*II sites of plasmid pBLCAT2 in place of the *tk* promoter. The plasmid was then cut either with *Bam*HI and *Kpn*I (which cuts in the polylinker downstream of the SV40 polyadenylation sequence) or with *Bgl*II and *Kpn*I. The two DNA fragments were gel purified and ligated to produce a plasmid with a duplicated copy of the oligonucleotide. The procedure was repeated to generate a plasmid with four copies. The DNA fragment containing the DR tetramer was then cut with *Bam*HI and *Bgl*II, gel purified, and subcloned into the *Bam*HI site upstream of the *tk* promoter in plasmid pBLCAT2 or downstream of the CAT gene in plasmid pVC(25S).

Mutagenesis. Site-directed in vitro mutagenesis was performed by the method of Kunkel (14), using a Muta-Gene kit (Bio-Rad). The uracil-containing single-stranded DNA template was prepared by transformation of the dUTPase- and uracil *N*-glycosylase-deficient *Escherichia coli* strain CJ236 with plasmid pVCE(1Z) and superinfection with the helper phage M13KO7 according to the manufacturer's recommendations. The mutagenic oligonucleotides were synthesized on an Applied Biosystems DNA synthesizer and were 18 to 24 nucleotides long. The mutant plasmids were sequenced by the dideoxynucleotide chain termination method, using Sequenase (U.S. Biochemical). Single- to triple-base substitution mutants were generated and tested for CAT expression in CA46 cells in at least four transfection experiments. To ensure that the effect seen on CAT activity was not due to unnoticed alterations in the plasmid sequence that may have occurred during the mutagenesis procedure, four mutant enhancer inserts were subcloned back into the original Vκ-CAT vector and tested for CAT activity. These control experiments confirmed that the effect on CAT expression resulted from the enhancer mutation (data not shown).

Cell culture and transfections. The human Burkitt lymphoma B-cell line CA46 (kindly provided by Ian Magrath, National Institutes of Health), the lymphoblastoid cell line SB (American Type Culture Collection [ATCC]), and the T-cell line Jurkat (ATCC) were grown in RPMI 1640 supplemented with 10% heat-inactivated fetal bovine serum (GIBCO). The murine myeloma S194 cell line (ATCC) and the human cervical carcinoma HeLa cell line (ATCC) were grown in Dulbecco modified Eagle medium supplemented with 10% heat-inactivated fetal bovine serum.

Transfections were performed by a DEAE-dextran procedure. Cells (5×10^6) were incubated in 1 ml of 137 mM NaCl–5 mM KCl–0.4 mM Na_2HPO_4–25 mM Tris–10 mM $MgCl_2$–10 mM $CaCl_2$ with 3 μg of supercoiled plasmid DNA and 200 μg of DEAE-dextran (Pharmacia) for 15 min at room temperature; then 5 ml of 60 μM chloroquine diphosphate in serum-free medium was added, and incubation continued for 30 min at 37°C. Cells were collected by centrifugation and resuspended in 15 ml of complete medium. Cells were transferred to 10-cm-diameter plates and cultured at 37°C for 48 to 72 h. Extracts were prepared by three rounds of

freeze-thawing in 0.25 M Tris (pH 7.4). CAT activity was assayed by the fluor-diffusion assay, using ^{3}H-acetyl coenzyme A as described by Neumann et al. (25). The data were normalized to the protein concentration in the extract. In some experiments, CAT activity was normalized against luciferase activity programmed by a cotransfected cytomegalovirus-luciferase plasmid (kindly provided by Vinay Jain, National Cancer Institute).

Electrophoretic mobility shift assays (EMSAs). Nuclear extracts were prepared by the method of Dignam et al. (6) except that KCl was used instead of NaCl in buffer C. Binding reaction mixtures (25 μl) contained 10 mM Tris (pH 7.4), 100 mM NaCl, 1 mM dithiothreitol, 1 mM EDTA, 4% glycerol, 80 μg of sonicated salmon sperm DNA per ml, nuclear extract (10 μg of protein), and 1 ng of ^{32}P-labeled probe. The probes were prepared by annealing complementary synthetic oligonucleotides in 150 mM NaCl and end labeled with [γ-^{32}P]ATP and T4 polynucleotide kinase; they were then subjected to purification on G50 spin columns (5 Prime-3 Prime). All components of the binding reaction mixtures, including competitor when specified, were mixed on ice, with the protein extract being added last. Binding reactions were performed at 20°C for 20 min, and the mixtures were then loaded onto a 5% polyacrylamide gel (30:1 acrylamide/bisacrylamide ratio) containing 25 mM Tris (pH 8.0), 25 mM boric acid, and 0.5 mM EDTA (0.25× TBE). The gel was preelectrophoresed for 60 min at 4°C before loading of the samples and then electrophoresed at 15 V/cm at 20°C. Gels were dried and exposed to XAR-5 film with an intensifying screen at −80°C.

In vivo genomic footprinting. In vivo DMS footprinting was performed on cultured HeLa cells and on lymphoid cells in suspension by the ligation-mediated PCR (LM-PCR) method of Mueller and Wold (21). For the adherent HeLa cells, the culture medium was replaced with medium containing 10% fetal bovine serum and 0.2% DMS, and cells were incubated at room temperature for 5 min. The cells were washed twice with phosphate-buffered saline (PBS) and detached by trypsin treatment. The cell suspension was diluted in 10 volumes of ice-cold PBS, and cells were collected by centrifugation. Lymphoid cells growing in suspension were resuspended in RPMI containing 10% fetal bovine serum at a concentration of 10^{8} cells per ml; DMS was added at a concentration of 0.1%, and cells were incubated for 10 min at room temperature. The reaction was quenched by addition of 10 volumes of ice-cold PBS; the mixture was then centrifuged and washed once with PBS. For both HeLa and lymphoid cells, DNA was prepared by incubating the cells overnight at 56°C in lysis buffer containing 1 mM Tris (pH 7.5), 400 mM NaCl, 2 mM EDTA, 0.2% sodium dodecyl sulfate, and 0.2 mg of proteinase K (GIBCO) per ml. After phenol-chloroform extraction, the DNA was precipitated in ethanol and redissolved in 10 mM Tris (pH 8.0)–1 mM EDTA. The DNA (50 to 100 μg) was dissolved in 1 M piperidine (Aldrich) in siliconized Eppendorf tubes and heated at 90°C for 30 min. The cleaved DNA was precipitated and collected by centrifugation. The pellet was dissolved in sterile water and lyophilized in a Speedvac concentrator twice before being dissolved in sterile water and quantitated by fluorometry, using the Hoechst 33258 dye. Base-specific DNA modification reactions were performed on 20 μg of plasmid pVCE(57T) as described by Maxam and Gilbert (18). The plasmid DNA was cleaved with piperidine and precipitated as described above for genomic DNA.

The genomic footprints were obtained by the LM-PCR method essentially as described by Pfeifer et al. (29). The Sequenase reaction was performed with 5 μg of genomic and 1 ng of plasmid DNA, respectively (these amounts were found to give comparable signals on the sequencing gel). Ligation of the oligonucleotide linker to the blunt-ended primer-extended molecules was performed as described previously (29). The DNA fragments were amplified with 2.5 U of *Taq* polymerase (*Taq* sequencing grade; Perkin Elmer Cetus) in a thermocycler with the following program: an initial denaturation step at 94°C for 3 min, 17 to 20 cycles (1 min at 94°C and 4 min at 70°C), and one final cycle (1 min at 94°C and 10 min at 70°C). For the labeling step, 5 pmol of end-labeled primer 3 was added in a labeling mix as described previously (29), and the samples were heated at 94°C for 4 min (to denature the DNA) and at 72°C for 12 min (to extend the radiolabeled primer) and were then chilled on ice. After phenol-chloroform extraction and ethanol precipitation, the DNA fragments were resuspended in 4 μl of loading buffer containing 80% formamide and 10 mM NaOH, heated at 90°C for 3 min, and separated on 80-cm-long sequencing gels containing 8% polyacrylamide and 7 M urea (Marathon gel mix; Bethesda Research Laboratories). The gels were preelectrophoresed at 1,000 V for 4 h, electrophoresed at 1,500 V for 14 h, wrapped, and exposed to XAR-5 film with an intensifying screen at −80°C.

RESULTS

Mapping of a B-cell-specific enhancer downstream of the human Cκ region. A 1,120-bp *Pst*I-*Sst*I fragment lying 12 kb downstream of the human Cκ gene was found to include sequence homologous to the recently described murine 3′κ enhancer (22). We verified the nucleotide sequence of the *Pst*I-*Sst*I fragment and compared it with the published murine sequence. Dot matrix comparison showed that the strongest sequence identities lay in the 5′ portion of a 1-kb *Sca*I-*Sst*I fragment. To establish that the sequence conservation of this fragment reflected the presence of a functional enhancer, the fragment was inserted in both orientations downstream of the bacterial CAT gene transcribed from a Vκ gene promoter. Enhancer activity was measured as the ability of the different enhancer constructs to induce transcription of the CAT gene after transient expression in the human kappa-producing Burkitt lymphoma cell line CA46. In different transfection experiments, the 1-kb fragment stimulated transcription 10- to 50-fold relative to the enhancerless control plasmid [Fig. 1, plasmid pVCE(57T)].

To define a minimal enhancer domain within this fragment, deletion derivatives were made by using exonuclease III digestion from both the *Sst*I end and the *Sca*I end of the insert by digesting the plasmids containing the two orientations of the inserted enhancer fragment. The plasmids from these two deletion series were tested for CAT expression and compared with the full-length enhancer construct. As expected, the most highly conserved 5′ region of the insert contained the enhancer activity. The results indicate that most of the enhancer activity lies within the 168-bp region bracketed by the deletion endpoints of plasmids 117X and 74W (Fig. 1). A 218-bp fragment overlapping this critical region was synthesized by PCR and inserted into the Vκ-CAT plasmid downstream of the CAT gene, yielding plasmid pVCE(1Z). Further 5′ and 3′ deletion plasmids were derived from pVCE(1Z) by exonuclease III digestion and tested for CAT activity. Results of these experiments confirmed the localization of the functional enhancer to 175 bp in the pVCE(1Z) insert (Fig. 1).

To explore the cell type specificity of the enhancer, we

TABLE 1. Activities of various enhancer constructs in different cell types

Construct	Promoter	Enhancer[a]	CAT activity[b]			
			B cells		T cells (Jurkat)	Epithelial cells (HeLa)
			CA46	SB		
1	Vκ	3'κ (57T)	14.2		1.0	
2	Vκ	3'κ (1Z)	25	1.6	2.4	1.0
3	Vκ	κ-intron	5.1		1.2	
4	Vκ	IgH	57		1.0	
5	SV40	SV40	9.8	8.7	4.9	1.8
6	SV40	3'κ (57T)	5.1	11.8	1.1	1.0
7	SV40	3'κ (1Z)	13.9		1.7	
8	*tk*	3'κ (1Z)	47	45	1.6	

[a] 57T, 1-kb 3'κ enhancer insert; 1Z, 218-bp PCR-generated 3'κ enhancer insert. The enhancer was positioned downstream of the CAT gene in all constructs except construct 8, in which the enhancer was inserted upstream of the *tk* promoter.

[b] Expressed as fold enhancement over the activity of an enhancerless reference plasmid.

transfected different human cell lines representing B lymphoid cells (CA46 and SB), a T-lymphoid cell (Jurkat), and cervical cells (HeLa). Since the Vκ promoter is also B-cell specific, we made a series of plasmids in which the SV40 promoter or the *tk* promoter was substituted for the Vκ promoter. Plasmids containing the κ-intron enhancer, the IgH enhancer, or the SV40 enhancer were also tested to compare the relative strengths of these enhancers. The 3'κ enhancer was able to stimulate transcription from the heterologous SV40 and *tk* promoters and, as expected, was active only in cells of the B lineage (Table 1, constructs 5 to 8). In CA46, plasmid pVCE(1Z) was consistently more active (about 2-fold) than plasmid pVCE(57T), which contains the original 1-kb enhancer fragment (constructs 1, 2, 6, and 7), about 5-fold more active than the κ-intron enhancer, and 2.3-fold weaker than the IgH enhancer (constructs 2 to 4). The 3'κ enhancer in plasmid 1Z (construct 2) was almost inactive in the SB lymphoblastoid B-cell line. However, this inactivity may in fact be due to the lack of activity of the Vκ promoter in this cell line, since the enhancer could stimulate transcription from either the SV40 promoter (construct 6) or the *tk* promoter (construct 8). The 1-kb enhancer was inactive in three human pre-B-cell lines (Nalm-16, Reh, and Km-3) and was active in several other Burkitt lymphoma cell lines as well as in three human myeloma cell lines, H929, RPMI 82226, and IM-9 (unpublished data).

In vivo genomic footprinting of the 3'κ enhancer. To further localize potential functional motifs, we searched for B-cell-specific protein binding in the 220-bp enhancer by using an in vivo footprinting technique (21). In this method, living cells are treated with DMS under conditions that result in partial methylation of N-7 residues of guanosine (G) residues (8); the location of methylated G's is determined by piperidine cleavage followed by LM-PCR and high-resolution electrophoresis (Fig. 2A). Close contact of a protein to the DNA can either decrease the DMS reactivity of G residues by tight binding within the major groove or enhance their reactivity, presumably by locally increasing the reagent concentration in hydrophobic patches (26). Footprinting experiments were performed on each of four cell lines (the CA46 and SB B-cell lines, the Jurkat T-cell line, and the HeLa cervical cell line) at least twice and using various concentrations of DMS to ensure that the observed modifications in G reactivities were reproducible.

Figure 2B shows the result of such an experiment in which the 220-bp 3'κ enhancer fragment was analyzed on both strands in the four cell lines. Only the central 120 nucleotides are shown, since no other footprints were detected in the rest of the sequence. Most instructive is a comparison of the reactivity of each G (measured by the intensity of the corresponding band) in the two B-cell lines CA46 and SB versus the two non-B-cell lines Jurkat (T cell) and HeLa (carcinoma). Multiple bands in the B-cell lines appear to be protected or enhanced compared with the bands from non-B-cell lines. The modified G's are clustered and identify four regions of B-cell-specific changes indicated by the four segments of DNA sequence in Fig. 2B. The two 3' regions (PU and HM) showing B-cell-specific alteration in DMS reactivity are homologous to functional motifs identified in the mouse enhancer and correspond to PU.1-like and HLH-binding sites. The two 5' sequences, DR and DS (downstream [from the DR] sequence), showing B-cell-specific footprints have not been identified as functional motifs in the mouse enhancer. However, their sequences are well conserved between mouse and human genes, and our transfection analysis with mutant enhancers shows that one, DR, is functional in the human enhancer (see below). The four motifs identified by in vivo footprinting as potentially important for the function of the enhancer were studied in detail as described below.

Identification of a new enhancer element. The most 5' of the protected regions is a nearly exact tandem repeat of a 12-bp sequence, ATAGCAAC(C/T)GTC, which we have designated DR. This motif shows a large B-cell-specific footprint that is unique for each of the two repeats and includes an enhancement on the lower strand in the upstream repeat. The downstream repeat shows more protected G's than does the upstream repeat (6 of 12 versus 2 of 12), and there is an additional protected G on the lower strand two nucleotides downstream of the repeat (Fig. 2B).

To test whether the DNA motifs that were identified by B-cell-specific in vivo footprints corresponded to functional elements, we made a series of mutant enhancers constructed by site-directed mutagenesis. Transfection of plasmids containing mutations in the DR motif into CA46 cells indicated that this element is critical for enhancer function. Mutants M3 and M4 decreased enhancer activity to 13 and 19%, respectively, of the wild-type level (Fig. 3A). Each of these mutants introduces a double substitution eliminating G's that show B-cell-specific protection in vivo and are located in the downstream part of DR. Two other mutations which alter the upstream part of the repeat, including the enhanced G on the lower strand, also reduced enhancer activity significantly (M18 and M31; 21 and 28%, respectively, of the wild-type level; Fig. 3A).

To further characterize the DR motif, we examined its ability to bind nuclear proteins in vitro. Double-stranded oligonucleotides were used as probes or as cold competitors in EMSAs. Incubation of a probe (DRL) containing the entire DR region with nuclear extract from the B-cell line CA46 led to several retarded bands (numbered 1 to 6 in Fig. 4A). These bands were specifically competed for by cold probe but not fully competed for by several mutated cold probes (DRLM1, DRM1-2, and DRM2) that had two nucleotide changes in the 3' repeat. A competitor oligonucleotide truncated at the 3' end (DR) failed to compete for complex 6 specifically (Fig. 4A, lane 5). In addition, a mutated competitor (DRLM2) with sequence alteration near the 3' end competed for all complexes but less efficiently than did the wild-type DRL sequence for complex 6 (lane 3). Both of

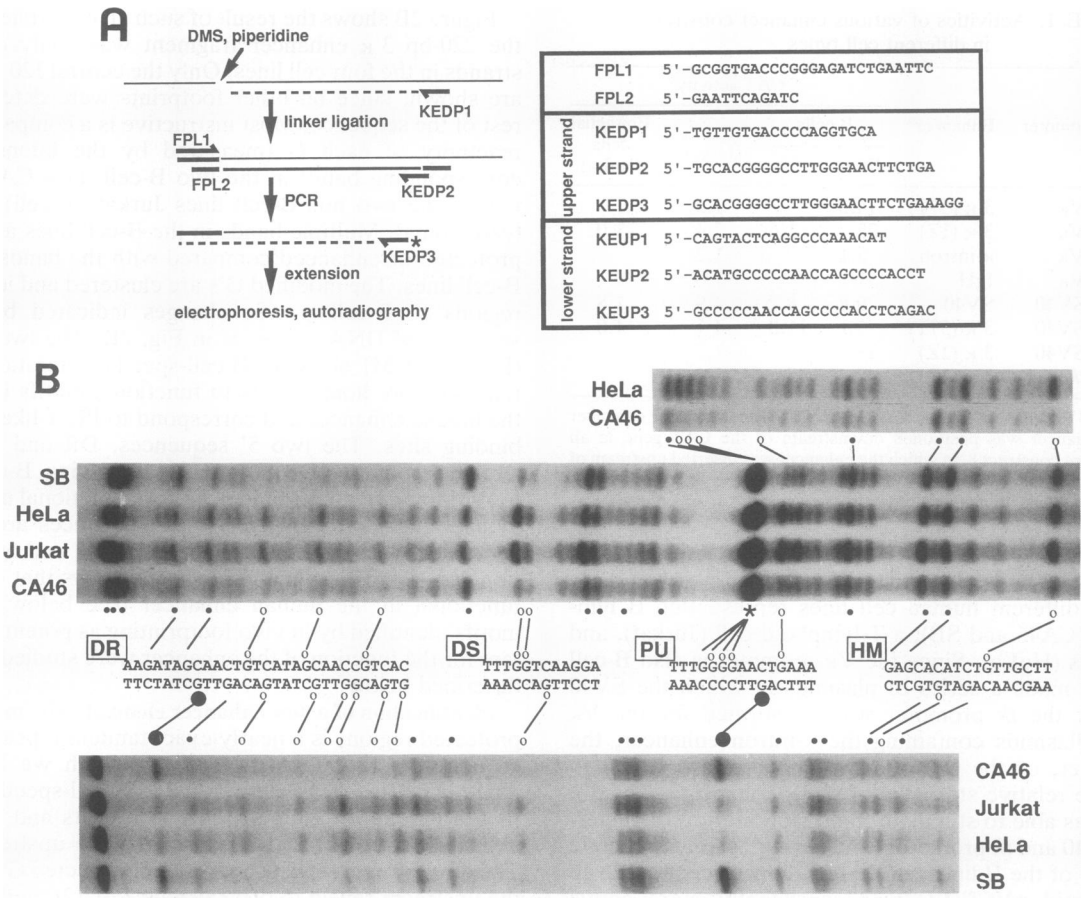

FIG. 2. Detection of B-cell-specific 3'κ enhancer-binding factors by in vivo DMS footprinting. (A) Outline of the LM-PCR procedure and sequences of the oligonucleotide primers. Oligonucleotides FPL1 and FPL2 were used to make the double-stranded footprinting linker, and FPL1 was paired with either KEDP2 or KEUP2 for PCR amplification of the upper or lower strand, respectively. (B) Assay in which Maxam-Gilbert sequencing reactions were performed on 1 ng of plasmid pVCE(1Z), using the LM-PCR procedure, and run next to the genomic samples to identify the bands corresponding to G's (not shown). Enhancer regions showing B-cell-specific changes in DMS reactivity are indicated by the nucleotide sequences for both strands. Guanosines are marked as follows: enhancement (large filled circles); protection (small open circles); and no change (small filled circles). The star indicates four G's that were collapsed by an electrophoresis artifact in the upper-strand gel. The corresponding region from another experiment is shown at the top.

these results suggest that the sequence at the 3' end of the probe may be important for the formation of complex 6.

In the 5' repeat, a mutation substituting a lower-strand G that showed a B-cell-specific enhancement in DMS footprinting left the fragment (DRM1) identical to the wild-type truncated motif (DR) in its ability to compete with labeled probe (Fig. 4A, lane 8), although the corresponding mutation in the 3' repeat (DRM2; lane 7) abolished competition of all bands. The apparent greater importance of the 3' repeat for in vitro protein binding may be related to the stronger methylation protection of this repeat in vivo than of the 5' repeat. An oligonucleotide spanning a portion of the human κ-intron enhancer conserved region (KICR) (7) with a 9-of-12-bp sequence identity (in reverse orientation) with the DR motif and an oligonucleotide (HM) containing the HLH-binding site both failed to compete with the DRL probe (lanes 9 and 10). Incubation of the DRL probe with various nuclear extracts showed a similar pattern of protein-DNA complexes in both B and T cells and the absence of complexes 1 to 3 in HeLa cells (Fig. 4B).

To test whether the DR motif alone could activate B-cell-specific transcription, we made plasmids containing a tetramer of an oligonucleotide spanning the repeat and extending two nucleotides further downstream to include all of the protected G's (see Materials and Methods). The tetramer was inserted either downstream of the CAT gene in the Vκ-CAT vector or upstream of the *tk* promoter in the *tk*-CAT vector; both constructs were tested for CAT expression in CA46 cells. Neither of the constructs programmed detectable CAT activity above that of the enhancerless constructs (data not shown).

We detected another region of DMS protection 3' of DR, which we have designated DS. This region includes two weakly protected G's on the upper strand and one strongly protected G on the lower strand. However, mutation of two of the protected G's in the DS region had no effect on enhancer activity (mutant M5; Fig. 3A). In addition, a DS oligonucleotide failed to bind nuclear factors in EMSAs (not shown). It therefore seems that the in vivo DMS footprint at this motif does not reflect the presence of a sequence-specific protein-DNA complex critical for enhancer function.

Functional characterization of the PU-like element. Moving 3' from the DR and DS sequences, the next motif showing

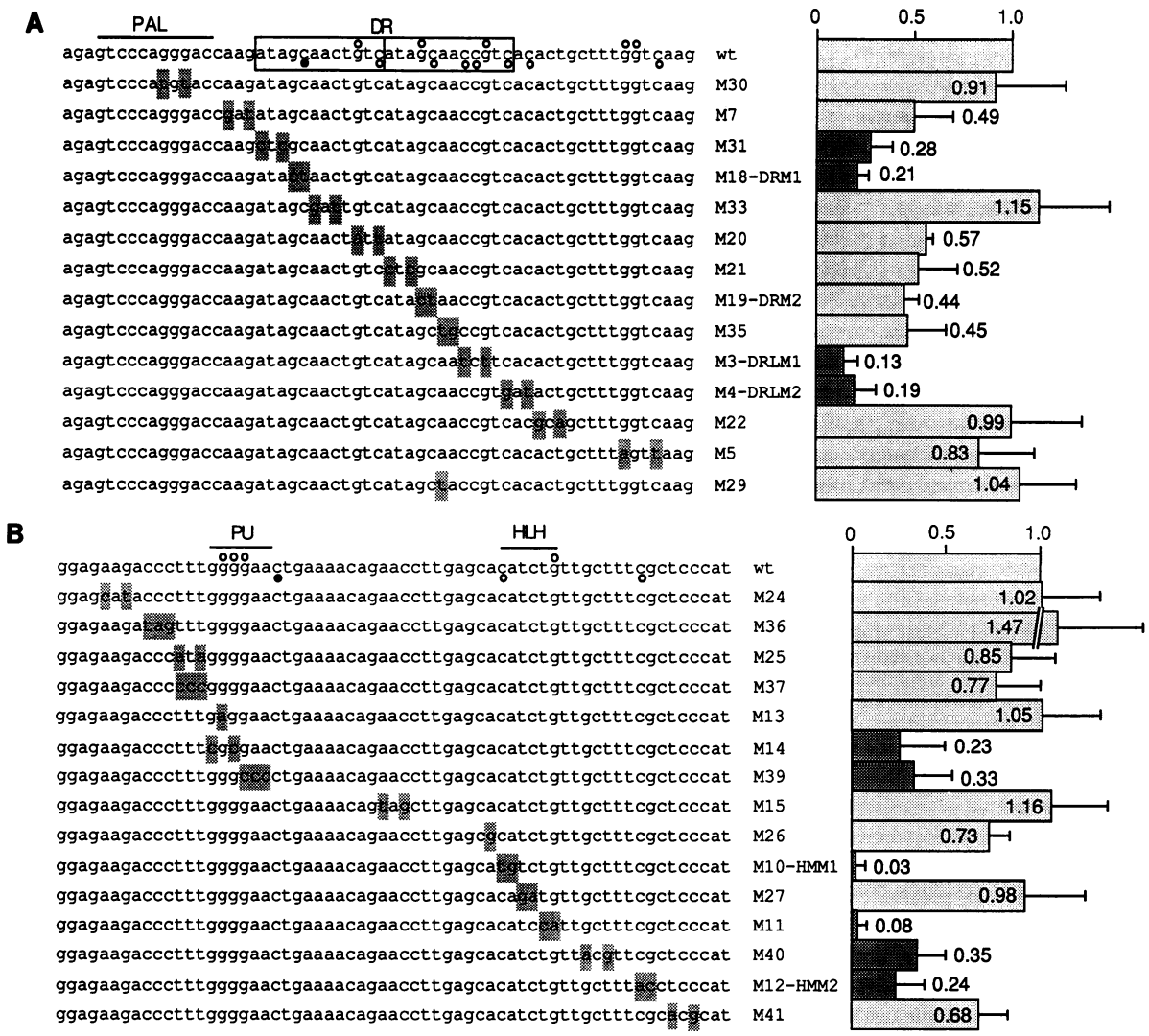

FIG. 3. Effects of specific mutations on the activity of the 3'κ enhancer. Plasmid pVCE(1Z) containing the 218-bp wild-type 3'κ enhancer (wt) and plasmids containing mutant enhancers generated by site-directed mutagenesis (M series) were tested for CAT activity in CA46 cells. The activity of each mutant relative to that of the wild-type enhancer (assigned value of 1.0) is indicated by bars and numbers in the bar graph and represents the average from at least four experiments; error bars indicate the standard deviation of the observed CAT activities. Beside the names of several mutant plasmids are given the names of corresponding mutant oligonucleotides used in EMSA experiments shown Fig. 4 to 6. The G's showing B-cell-specific changes in DMS reactivity in genomic footprinting are indicated as open (protection) or filled (enhancement) circles; a symbol above the sequence represents to a G in the upper strand, while a symbol below the sequence represents a G in the lower strand. Shaded areas in the sequence indicate the substituted nucleotides in each mutant. (A) Portion of the enhancer including the DR element (boxed); (B) portion of the enhancer including the PU and HLH motifs.

B-cell-specific DMS protection in vivo is the sequence TTTGGGGAA. The protected bases are embedded in a DNA sequence similar to the PU box sequence in the murine 3'κ enhancer (TTTGAGGAA) (30) and identical to the recently described μB element in the IgH enhancer (TT TGGGGAA) (16, 24). On the upper strand, the three most downstream G's of this motif, as well as a G 3 bp downstream of the motif, show B-cell-specific protection, while a single G on the lower strand is enhanced. In the experiment illustrated in Fig. 2B, an electrophoresis artifact in the upper-strand gel collapsed the bands corresponding to the four G's of the upper strand; the corresponding region from another experiment is shown at the top to demonstrate the protected G's.

To identify any functionally important residues in this motif, we generated clustered mutations of two or three nucleotides, some of which were identical to the mutations used to characterize the μB element of the IgH enhancer. Mutation M37 changes the three T's of the sequence into C's and had only a modest effect on enhancer activity (77% of the wild-type level; Fig. 4B), whereas the same changes in the μB element of the IgH enhancer were reported to completely abolish its activity (24). Mutation of two of the four G's (one of which shows B-cell-specific protection in vivo) was the most detrimental PU mutant tested (M14; 23% of the wild-type level), whereas mutation of three of the G's in the μB motif was reported to have no effect on enhancer activity. Finally, mutation M39, which changes the last three purines to C's, decreased enhancer activity to 33% (Fig. 3B), while the same mutation in μB decreased the activity of the

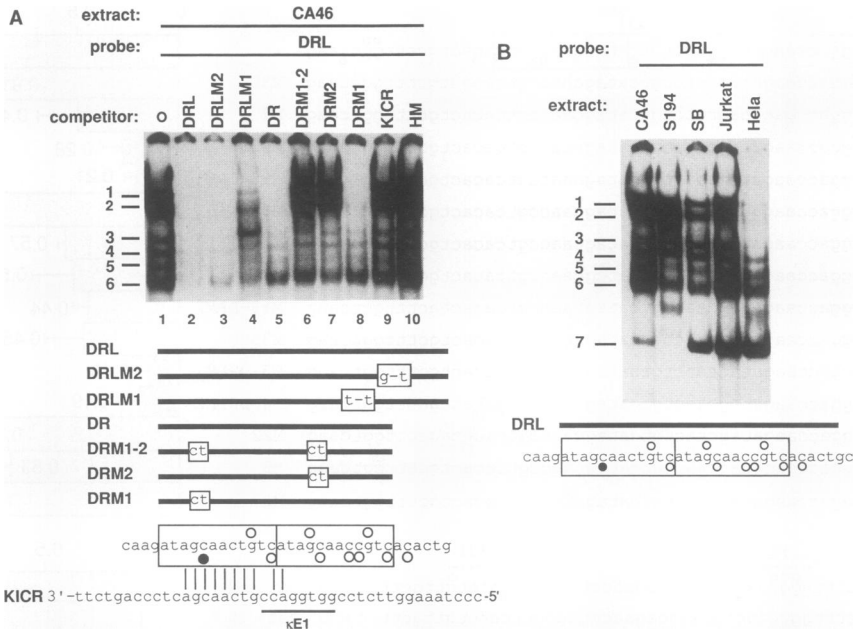

FIG. 4. Identification of nuclear proteins binding to the 3′κ enhancer DR motif in vitro. DR-binding factors were detected in EMSA, using a probe (DRL) with the sequence shown at the bottom. G's showing B-cell-specific protection (open circles) or enhancement (closed circles) in genomic DMS footprinting are indicated. Here and in Fig. 5 and 6, the free probe, which was run near the bottom of long gels in order to maximize separation of slower-moving bands, has been cut off the photograph. (A) Competition experiment using B-cell (CA46) nuclear extract. Competitors were added in 100-fold molar excess. Substituted nucleotides in competitors are boxed. The sequence (in reverse orientation) of the KICR oligonucleotide is shown at the bottom; the κE1 site is indicated. (B) Distribution of the DR-binding factors in various cell types.

IgH enhancer to 7% of the wild-type level. Thus, in the 3′κ enhancer, the critical residues comprise the stretch of six purines (GGGGAA) and include three G's showing B-cell-specific protein binding in vivo.

Incubation of a labeled probe spanning the PU region with B-cell nuclear extracts produced several protein-DNA complexes, three of which (complexes 1, 2, and 3) were partially competed for by cold probe or by an oligonucleotide containing the murine sequence GAGGAA (Fig. 5A). Complexes 2 and 3 were not competed for by a mutant oligonucleotide in which three of the four G's of the PU box were converted to C's, but this mutant oligonucleotide could compete for complex 1 (Fig. 5A, lane 4). The three specific complexes also showed a different cell type distribution. Complex 1 was present in all cell lines tested, whereas complex 3 was restricted to B cells (Fig. 5B). Complex 2 was only slightly competed for and probably corresponds to both specific and nonspecific protein-DNA binding.

Analysis of the HLH-binding site. The last sequence showing B-cell-specific DMS protection in genomic footprinting includes the sequence CATCTG identified as HM in Fig. 2B. The G's on both strands of this palindromic motif show weak protection in B cells. In addition, a G on the lower strand eight nucleotides downstream of the motif also showed weak protection in B cells (not shown). Mutations of this element were the most detrimental for enhancer function. Mutants M10 and M11 decreased enhancer activity to 3 and 8%, respectively, of the control level (Fig. 3B). Each of these mutants has a 2-bp transversion affecting either one of the two (underlined) distal pairs of nucleotides in the CATCTG sequence, which has been described as the core DNA-binding sequence of the family of HLH transcription factors (3). Mutation of the two central pyrimidines did not affect enhancer activity (mutant M27; Fig. 3B). A 2-bp mutation including the additional G that shows B-cell-specific protection (located 8 bp downstream of the HM motif on the lower strand) decreased enhancer activity to 24% of the wild-type level (M12; Fig. 3B), and mutation of two residues between the core motif and this protected G also reduced enhancer

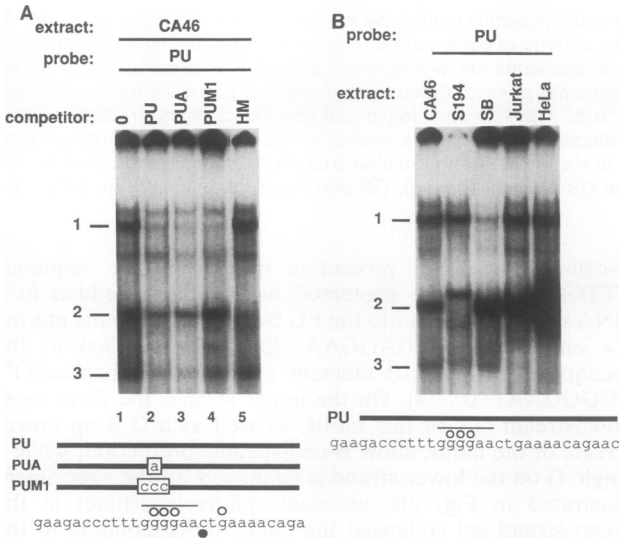

FIG. 5. Identification of nuclear proteins binding to the 3′κ enhancer PU box element. Symbols are identical to those in Fig. 4. (A) Competition experiment; (B) cell type distribution of the PU-binding factors.

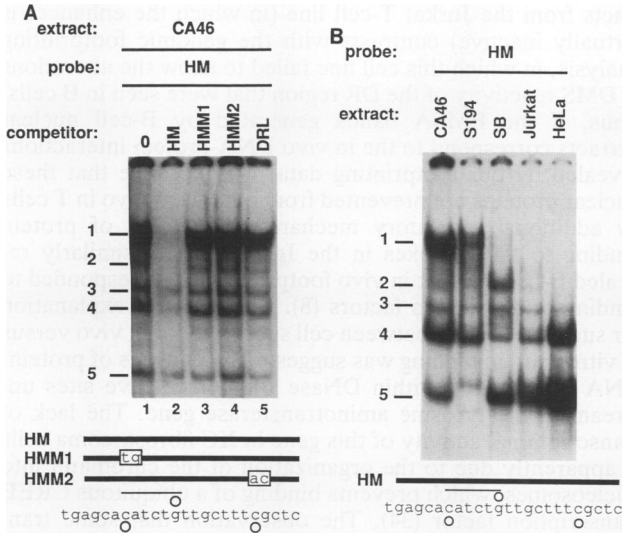

FIG. 6. Identification of nuclear proteins binding to the 3′κ enhancer HLH-binding element. Symbols are identical to those in Fig. 4. (A) Competition experiment; (B) cell type distribution of the HLH-binding factors.

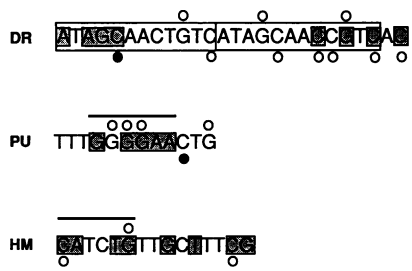

FIG. 7. Summary of functional and protein-DNA binding data for the human 3′κ enhancer motifs. Guanosines showing B-cell-specific changes in DMS reactivity are indicated by open (protection) or closed (enhancement) circles above the sequence for the upper strand and below the sequence for the lower strand. The residues important for enhancer function and/or binding of nuclear proteins in vitro are in shaded boxes. The 11/12-bp DR is boxed, and the consensus binding sites for both the PU.1 and HLH transcription factors are shown by lines above their corresponding sequences.

activity to 35% of the wild-type level (M40; Fig. 3B). The effect of these mutations correlates with the inability of the corresponding mutant oligonucleotides to compete for binding of nuclear factors to an HM oligonucleotide in vitro (see below).

In EMSA, a probe including the HM motif led to several retarded bands, numbered 1 to 5, upon incubation with B-cell nuclear extract (Fig. 6A). The top two complexes 1 and 2 were specifically competed for by cold probe (Fig. 6A, lane 2) but not by two mutated cold probes changing either the 5′ two nucleotides of the core CATCTG sequence (mutant HMM1; lane 3) or two nucleotides including the protected G 8 bp downstream of the core motif (mutant HMM2; lane 4). A cold probe containing the DR motif failed to compete with probe HM, further demonstrating the specificity of complexes 1 and 2 (lane 5). Upon incubation with nuclear extracts from various cell lines, either complex 1 or complex 2 was present in the B-cell lines CA46, S194, and SB (Fig. 6B), while both complexes were absent in HeLa cells.

DISCUSSION

A conserved sequence similar to the mouse 3′κ enhancer has been found to lie 12 kb downstream of the human Cκ exon gene (22). We have examined this human DNA sequence for enhancer activity. Upon transfection into B-cell lines, a 1-kb *Sca*I-*Sst*I fragment stimulated transcription of the CAT gene from a Vκ promoter in an orientation-independent manner. The results from our transfection experiments in various human cell lines show that, like the murine enhancer (30), the human enhancer is active only in mature B cells and is about fivefold stronger than the κ-intron enhancer. Deletion analysis revealed that the core enhancer is contained in a 175-bp fragment corresponding to the sequence most highly conserved (92%) between human and mouse genes. In CA46 cells and in the Jurkat T-cell line (in which the enhancer is only slightly active), we found that a 218-bp insert centered on the core enhancer was consistently more active (twofold) than the 1-kb *Sca*I-*Sst*I fragment; this finding may reflect the presence of negative regulatory elements outside of the core enhancer. A negative regulatory element has been recently identified downstream of the murine core enhancer and was shown to repress enhancer activity about 10-fold in murine pre-B cells. This sequence binds a zinc finger protein (called NF-E1, YY-1, or δ) and shows homology to the IgH enhancer μE1 site (27). The same ubiquitous protein (UCRBP) was recently found to bind to the upstream conserved region of the Moloney murine leukemia virus long terminal repeat and mediate negative regulation of virus promoter activity (9). Although the negative regulation previously attributed to this element was not reported to function in mature murine B cells (27), our observations suggest that it may function in the human CA46 line. Alternatively, the consistently greater enhancer activity of the 218-bp insert than of the 1-kb insert might reflect a different, as yet unidentified negative element in the longer insert.

Using genomic footprinting and functional assays with mutant enhancers, we have characterized three positive regulatory elements that show B-cell-specific protein binding in vivo. Figure 7 summarizes the footprinting and functional data for these three motifs. Although the human enhancer functions similarly to the murine homolog, we found a significant difference in the human enhancer by identifying a third functional element overlapping with a 11/12-bp direct repeat, in addition to the PU box and HLH-binding motifs identified in the mouse enhancer. Although the DR sequence is well conserved in the mouse, deletions overlapping the DR element had no effect on the activity of the mouse enhancer in MPC11 plasmacytoma cells as reported in studies by Meyer et al. (20). Because the murine enhancer in this region differs from the human sequence by one nucleotide (an A→T transversion), we made a mutant enhancer in which the mouse sequence had been restored. However, this mutant was identical to the wild-type enhancer in its ability to stimulate transcription (Fig. 4A, mutant M29). Since in the study of Meyer et al. the enhancer was located upstream of a β-globin promoter, we also tested the effect of mutation of the DR motif on the activity of the enhancer inserted upstream of the β-globin promoter. Mutation of DR decreased enhancer activity of these constructs to 10 to 20% of the wild-type level, ruling out the possibility that the function of the DR element was position or promoter dependent

(not shown). Mutation of DR also reduced the activity of the enhancer in the murine S194 cell line (data not shown), and mobility shift assays with S194 nuclear extracts revealed a pattern of DR-binding factors indistinguishable from that obtained with nuclear extracts from human B cells (Fig. 6B). The possibility still exists, however, that the *trans*-acting factors mediating the enhancer activity of the DR element are functional in S194 but not in MPC11, the cell line used in the study of the murine enhancer.

No similarity between the DR element and other enhancer motifs was detected in a computer search of DNA regulatory elements (10). A 9-of-12-bp homology (although in reverse orientation) was found with a region of the human KICR which overlaps the κ-intron enhancer (7). However, an oligonucleotide encompassing this KICR region failed to compete for binding of nuclear proteins with the DR probe in a mobility shift assay. A tetramer of the DR motif failed to stimulate transcription from two different promoters (Vκ and *tk*), suggesting that the DR element alone does not act as a transcriptional activator. This finding is consistent with results of similar experiments with the murine enhancer, in which a tetramer of a sequence overlapping the DR motif also failed to stimulate transcription from the *tk* promoter (30).

Multiple specific protein-DNA complexes were detected upon incubation of a DR sequence with various nuclear extracts. Some of these complexes were lymphoid cell specific, and others were also present in HeLa cells. In addition, various mutant DR oligonucleotides failed to compete efficiently with the DR probe for the formation of specific subsets of these complexes. Together, these results suggest that several distinct nuclear factors, some lymphoid cell specific and others more widely distributed, bind to the DR motif.

Although the competition experiments with mutant oligonucleotides clearly demonstrated sequence-specific binding to the DR sequence, our analyses have not yet suggested a simple model relating a specific EMSA band with enhancer function. One can hypothesize that nucleotides near the 3′ end of the DR motif are important both for the formation of complex 6 and for enhancer function. The role of these nucleotides in complex 6 is suggested by the fact that the truncated oligonucleotide competitors DR, DRM1, and DRM2 all failed to compete for this band. Furthermore, the competitor oligonucleotides DRLM1 and DRLM2, with mutations near the 3′ end, failed to compete for this band (compare lane 2 of Fig. 4A with lanes 3 and 4), and corresponding mutations in our CAT constructs inhibited enhancer activity (Fig. 3A). However, it is puzzling that the functional inhibition observed with the DRLM2 mutant plasmid was substantial (about 80%), whereas the decrease in EMSA competition caused by this mutation was relatively slight. An additional puzzling observation regarding the functional importance of the EMSA bands concerns mutations DRM1 and DRM2. Mutation DRM1 has little effect on the ability to compete for binding of the complexes represented by the intense EMSA bands 1 and 2 (Fig. 4A, lane 8 versus lane 5), yet this mutation inhibits enhancer function by about 80%. On the other hand, mutation DRM2 causes somewhat less functional inhibition but almost completely blocks competition for EMSA bands 1 and 2 (Fig. 4A, lane 7). Clearly, further experiments using additional mutations in EMSA experiments and transfected plasmids will be necessary to clarify the relationship between the EMSA complexes and enhancer function.

The presence of the DR-binding factor(s) in nuclear extracts from the Jurkat T-cell line (in which the enhancer is virtually inactive) contrasts with the genomic footprinting analysis, in which this cell line failed to show the alterations in DMS reactivity of the DR region that were seen in B cells. Thus, if the EMSA bands generated by B-cell nuclear extracts correspond to the in vivo DNA-protein interactions revealed by our footprinting data, it is possible that these nuclear proteins are prevented from binding in vivo in T cells by additional regulatory mechanisms. Studies of protein binding to the E boxes in the IgH enhancer similarly revealed B-cell-specific in vivo footprints that corresponded to binding of ubiquitous factors (8). One possible explanation for such differences between cell specificity of in vivo versus in vitro protein binding was suggested by analysis of protein-DNA interactions within DNase I-hypersensitive sites upstream of the tyrosine aminotransferase gene. The lack of transcriptional activity of this gene in XC fibrosarcoma cells is apparently due to the organization of the chromatin into nucleosomes, which prevents binding of a ubiquitous CREB transcription factor (34). The observation that some transcription factors may bind to their recognition sequence only after removal of positioned nucleosomes has also been made previously in other systems (1, 4, 32). These results and ours emphasize the necessity of direct in vivo analysis of protein-DNA interactions to verify conclusions derived from in vitro studies. The intriguing question of whether or not such mechanisms operate to regulate the access of the DR-binding factors to their binding sites in B and T cells awaits further experimentation.

The 3′κ enhancer motif that we designate PU is identical in sequence to the recently identified μB element in the IgH enhancer (16, 24) and also resembles the consensus recognition sequence for DNA-binding factors containing the Ets domain, an 85-amino-acid region conserved in a family of transcription factors, including PU.1 and the *ets-1* proto-oncogene (13). The PU homolog in the murine enhancer binds the PU.1 protein (hence our designation of this element in the human enhancer) (31). Our analysis indicates that mutation of the three T's in the TTTGGGGAA sequence to CCC had a minimal effect on 3′κ enhancer activity, whereas the identical mutation abolished μB activity (24). Furthermore, mutation of the PU element in the human enhancer so that it matched exactly the murine sequence (TTTGAGGAA) had no effect on enhancer activity (Fig. 3B) and in vitro binding of nuclear proteins (Fig. 5A). In contrast, mutations that altered the GGAA sequence thought to be critical for DNA binding by Ets domain proteins inhibited both enhancer function (Fig. 3B) and nuclear protein binding (Fig. 5A). It is therefore likely that the TTTGGGGAA sequence in the human 3′κ enhancer binds a PU.1-like protein rather than to NF-μB. Recently PU.1 was found to recruit an additional protein, NF-EM5, to bind just downstream of the PU homolog in the murine 3′κ enhancer (31). Interestingly, the binding of this factor is dependent on a G residue 3 bp downstream of the GGAA motif, a position where we find a B-cell-specific protection in our in vivo footprinting. It seems possible that this protection reflects the binding of a similar protein in the human enhancer.

The third functional element of the 3′κ enhancer contains the sequence CATCTG, which matches the consensus recognition sequence for transcription factors of the HLH type (3, 5, 23). The HLH protein motif is highly conserved in a variety of nuclear proteins, including E-box-binding proteins (11), members of the Myc family, and transcription factors that induce muscle differentiation (23). This motif allows the formation of homo- or heterodimers between different mem-

bers of the HLH proteins, which can result in an increase in their DNA binding affinity. In addition, negative regulation of HLH factors can be mediated by HLH proteins that form heterodimers but lack a DNA-binding region, such as the HLH protein Id (3). Id was found to inhibit transcriptional activation by several known HLH proteins and to suppress the activity of the murine 3'κ enhancer presumably by a similar mechanism (30). We found a good correlation between protein binding in vivo to the HM motif as detected by genomic footprinting and the effect of mutations of the protected nucleotides on both enhancer activity and binding of B-cell-specific nuclear factors in vitro. Our results show that the critical residues are the underlined nucleotides in the sequence CATCTG, in agreement with the described flexibility of the internal nucleotides in the recognition sequence of various HLH proteins (5). Genomic footprinting showed the presence of a B-cell-specific protected G on the lower strand 8 bp downstream of the core motif; and mutation of the corresponding residue decreased enhancer activity, suggesting the possible presence of an additional binding factor (Fig. 7). However, in competition experiments in EMSA, this mutation inhibited binding of the HLH factor(s) to the same extent as did a mutation in the core sequence itself. We therefore favor the interpretation that in the context of the 3'κ enhancer, the sequence recognized by the HLH factor(s) extends 8 bp further downstream of the (core) CATCTG motif, although we cannot exclude the possibility that binding of the HLH factor to this motif depends on the adjacent binding of another factor through protein-protein interaction.

Our data indicate that, like many enhancers, the 3'κ enhancer is composed of several sequence motifs that bind to sequence- and tissue-specific nuclear factors. In its lack of apparent redundancy, the 3'κ enhancer resembles the intron κ enhancer rather than the intron heavy-chain enhancer, in which mutations in most of the individual motifs have little effect on enhancer function (15). Further analysis will be necessary to clarify the basis for the apparent cooperativity of the three motifs of the 3'κ enhancer, the reasons for the reported absence of DR motif activity in the murine 3'κ enhancer homolog, and the nature of the DNA-binding nuclear proteins that interact with each motif.

ACKNOWLEDGMENTS

We are most grateful to Mary Malarkey for excellent technical assistance in plasmid construction and sequencing, and we thank Andrew Larner and Steve Bauer for helpful comments.

REFERENCES

1. **Almer, A., H. Rudolph, A. Hinnen, and W. Horz.** 1986. Removal of positioned nucleosomes from the yeast PHO5 promoter upon PHO5 induction releases additional upstream activating DNA elements. EMBO J. **5**:2689–2696.
2. **Benezra, R., R. L. Davis, D. Lockshon, D. L. Turner, and H. Weintraub.** 1990. The protein Id: a negative regulator of helix-loop-helix DNA binding proteins. Cell **61**:49–59.
3. **Blackwell, T. K., and H. Weintraub.** 1990. Differences and similarities in DNA-binding preferences of MyoD and E2A protein complexes revealed by binding site selection. Science **250**:1104–1110.
4. **Cordingley, M. G., A. T. Riegel, and G. L. Hager.** 1987. Steroid-dependent interaction of transcription factors with the inducible promoter of mouse mammary tumor virus in vivo. Cell **48**:261–270.
5. **Dang, C. V., C. Dolde, M. L. Gillison, and G. J. Kato.** 1992. Discrimination between related DNA sites by a single amino acid residue of Myc-related basic-helix-loop-helix proteins. Proc. Natl. Acad. Sci. USA **89**:599–602.
6. **Dignam, J. D., P. L. Martin, B. S. Shastry, and R. G. Roeder.** 1983. Eukaryotic gene transcription with purified components. Methods Enzymol. **101**:582–599.
7. **Emorine, L., M. Kuehl, L. Weir, P. Leder, and E. E. Max.** 1983. A conserved sequence in the immunoglobulin J_κ-C_κ intron: possible enhancer element. Nature (London) **304**:447–449.
8. **Ephrussi, A., G. M. Church, S. Tonegawa, and W. Gilbert.** 1985. B lineage-specific interactions of an immunoglobulin enhancer with cellular factors in vivo. Science **227**:134–140.
9. **Flanagan, J. R., K. G. Becker, D. L. Ennist, S. L. Gleason, P. H. Driggers, B.-Z. Levi, E. Appella, and K. Ozato.** 1992. Cloning of a negative transcription factor that bind to the upstream conserved region of Moloney murine leukemia virus. Mol. Cell. Biol. **12**:38–44.
10. **Ghosh, D.** 1990. A relational database of transcription factors. Nucleic Acids Res. **18**:1749–1756.
11. **Henthorn, P., M. Kiledjian, and T. Kadesch.** 1989. Two distinct transcription factors that bind the immunoglobulin enhancer μE5/κE2 motif. Science **247**:467–470.
12. **Kadesch, T.** 1992. Helix-loop-helix proteins in the regulation of immunoglobulin gene transcription. Immunol. Today **13**:31–36.
13. **Karim, F. D., et al.** 1990. The ETS-domain: a new DNA-binding motif that recognizes a purine-rich core DNA sequence. Genes Dev. **4**:1451–1453.
14. **Kunkel, T. A.** 1985. Rapid and efficient site-specific mutagenesis without phenotypic selection. Proc. Natl. Acad. Sci. USA **82**:488–492.
15. **Libermann, T. A., and D. Baltimore.** 1991. Transcriptional regulation of immunoglobulin gene expression, p. 399–421. *In* P. Cohen and J. G. Foulkes (ed.), The hormonal control regulation of gene transcription. Elsevier Science Publishers B. V. (Biomedical Division), Amsterdam.
16. **Libermann, T. A., M. Lenardo, and D. Baltimore.** 1990. Involvement of a second lymphoid-specific enhancer element in the regulation of immunoglobulin heavy-chain gene expression. Mol. Cell. Biol. **10**:3155–3162.
17. **Luckow, B., and G. Schütz.** 1987. CAT constructions with multiple unique restriction sites for the functional analysis of eukaryotic promoter and regulatory elements. Nucleic Acids Res. **15**:5490.
18. **Maxam, A. M., and W. Gilbert.** 1980. Sequencing end-labeled DNA with base-specific chemical cleavages. Methods Enzymol. **65**:499–560.
19. **Meyer, K. B., and M. S. Neuberger.** 1989. The immunoglobulin κ locus contains a second, stronger B-cell-specific enhancer which is located downstream of the constant region. EMBO J. **8**:1959–1964.
20. **Meyer, K. B., M. J. Sharpe, M. A. Surani, and M. S. Neuberger.** 1990. The importance of the 3'-enhancer region in immunoglobulin κ gene expression. Nucleic Acids Res. **18**:5609–5615.
21. **Mueller, P. R., and B. Wold.** 1989. In vivo footprinting of a muscle specific enhancer by ligation mediated PCR. Science **246**:780–786.
22. **Muller, B., H. Stappert, and M. Reth.** 1990. A physical map and analysis of the murine Cκ-RS region show the presence of a conserved element. Eur. J. Immunol. **20**:1409–1411.
23. **Murre, C., et al.** 1989. Interactions between heterologous helix-loop-helix proteins generate complexes that bind specifically to a common DNA sequence. Cell **58**:537–544.
24. **Nelsen, B., T. Kadesch, and R. Sen.** 1990. Complex regulation of the immunoglobulin μ heavy-chain gene enhancer: μB, a new determinant of enhancer function. Mol. Cell. Biol. **10**:3145–3154.
25. **Neumann, J., C. A. Morency, and K. O. Russian.** 1987. A novel rapid assay for chloramphenicol acetyltransferase gene expression. BioTechniques **5**:444–448.
26. **Ogata, R. T., and W. Gilbert.** 1978. An aminoterminal fragment of lac repressor binds specifically to lac operator. Proc. Natl. Acad. Sci. USA **75**:5851–5854.
27. **Park, K., and M. L. Atchison.** 1991. Isolation of a candidate repressor/activator, NF-E1 (YY-1,δ), that binds to the immunoglobulin κ3' enhancer and the immunoglobulin heavy-chain μE1

site. Proc. Natl. Acad. Sci. USA **88**:9804–9808.
28. **Pettersson, M., and W. Schaffner.** 1987. A purine-rich DNA sequence motif present in SV40 and lymphotropic papovavirus binds a lymphoid-specific factor and contributes to enhancer activity in lymphoid cells. Genes Dev. **1**:962–972.
29. **Pfeifer, G. P., S. D. Steigerwald, P. R. Mueller, B. Wold, and A. D. Riggs.** 1989. Genomic sequencing and methylation analysis by ligation mediated PCR. Science **246**:810–813.
30. **Pongubala, J. M. R., and M. L. Atchison.** 1991. Functional characterization of the developmentally controlled immunoglobulin kappa 3′ enhancer: regulation by Id, a repressor of helix-loop-helix transcription factors. Mol. Cell. Biol. **11**:1040–1047.
31. **Pongubala, J. M. R., S. Nagulapalli, M. J. Klemsz, S. R. McKercher, R. A. Maki, and M. L. Atchison.** 1992. PU.1 recruits a second nuclear factor to a site important for immunoglobulin κ 3′ enhancer activity. Mol. Cell. Biol. **12**:368–378.
32. **Reik, A., G. Schütz, and F. A. Stewart.** 1991. Glucocorticoids are required for establishment and maintenance of an alteration in chromatin structure: induction leads to a reversible disruption of nucleosomes over an enhancer. EMBO J. **10**:2569–2576.
33. **Seidman, J., E. Max, and P. Leder.** 1979. A κ immunoglobulin gene is formed by site-specific recombination without further somatic mutation. Nature (London) **280**:370–375.
34. **Weih, F., D. Nitsch, A. Reik, G. Schütz, and P. B. Becker.** 1991. Analysis of CpG methylation and genomic footprinting at the tyrosine aminotransferase gene: DNA methylation alone is not sufficient to prevent protein binding in vivo. EMBO J. **10**:2559–2567.